Heliyon 10 (2024) e30996

Contents lists available at ScienceDirect

Heliyon

journal homepage: www.cell.com/heliyon

Research article

Dimensional accuracy and surface characteristics of complete-arch cast manufactured by six 3D printers☆

Mi-Young Sim [a], June-Beom Park [b], Deok-Yeoung Kim [c], Hae-Young Kim [d], Ji-Man Park [e,*]

[a] Department of Orthodontics and Dentofacial Orthopedics, Tsurumi University School of Dental Medicine, Yokohama, Japan
[b] Tsurumi University School of Dental Medicine, Yokohama, Japan
[c] Department of Prosthodontics School of Dentistry, Seoul National University, Seoul, Republic of Korea
[d] Department of Health Policy and Management, College of Health Science & Department of Public Health Sciences, Graduate School, and BK21 Four R&E Center for Learning Health Systems, Korea University, Seoul, Republic of Korea
[e] Department of Prosthodontics & Dental Research Institute, School of Dentistry, Seoul National University, Seoul, Republic of Korea

ARTICLE INFO

Keywords:
Low viscosity
Photopolymerization resin
Resolution
3D printing principle

ABSTRACT

Objective: This in vitro study aimed to quantitatively and qualitatively evaluate and compare the horizontal and vertical accuracies of complete-arch casts produced by six 3D printers with different printing principles and resolutions using a low-viscosity resin material.
Methods: A reference cast was designed by CAD software. The 3D printers used were DLPa (Asiga MAX), DLPk (cara Print 4.0), LCD2o (Ondemand 2 K Printer), LCD2p (Photon Mono X), LCD4s (SONIC 4 K), and SLA (ZENITH U). Ten casts were printed for each 3D printer using a low-viscosity resin. The accuracy of each printed cast was evaluated using shell-to-shell deviations, 12 linear, one angular, and five height deviations, with a reference cast as the control. The surface features of the casts were examined using field-emission scanning electron microscopy (FE-SEM) and digital cameras.
Results: The evaluation of shell-to-shell deviation revealed that DLPa and SLA printers exhibited low trueness values, whereas LCD printers displayed high trueness values. Among the LCD printers, LCD4s and LCD2o exhibited the lowest and highest trueness values, respectively. DLPa printers showed lower trueness values for intercanine and intermolar distances, whereas LCD printers generally demonstrated high trueness values. However, LCD4s exhibited similar trueness values to those of SLA and DLPk. The height deviation was smallest in the anterior area, whereas the largest height deviation occurred in the canine teeth. The surface characteristics indicated that the SLA casts had greater light reflection and blunt canine tips. The FE-SEM observations highlighted that the LCD and DLP printers exhibited varying layer characteristics, with some presenting rough and uneven borders in the anterior lingual area.
Significance: The accuracy of 3D printed casts varied among the 3D printer groups: DLPa and SLA were accurate for shell-to-shell deviation, with DLPa being the most accurate for linear and angular deviations. Regardless of the XY resolution, the DLP printers outperformed the LCD printers. Among the LCD group of 3D printers, higher-resolution LCD4s demonstrated increased

☆ Supported by the Korea Medical Device Development Fund grant funded by the Korea government (Project Number:202011A02).
* Corresponding author. Department of Prosthodontics & Dental Research Institute School of Dentistry, Seoul National University 101 Daehak-ro, Jongno-gu, Seoul Republic of Korea.
E-mail address: jimarn@gmail.com (J.-M. Park).

https://doi.org/10.1016/j.heliyon.2024.e30996
Received 9 October 2023; Received in revised form 19 March 2024; Accepted 9 May 2024
Available online 11 May 2024

accuracy. The SLA exhibited soft layer borders in the FE-SEM owing to its laser spot characteristics and prominent light reflection in the digital camera images.

1. Introduction

Current popular additive manufacturing technologies in the dental field include the Stereolithography Apparatus (SLA), digital light processing (DLP), and liquid crystal display (LCD), which use photocuring vat-polymerization techniques. SLA technology involves scribing a laser beam emitter, which requires a significant amount of time for 3D printing. A DLP printer is equipped with complex components such as a DLP engine, which makes it expensive. Both these types of 3D printers have been extensively used in clinical settings. Owing to the large number of models printed for the production of clear aligners in the field of orthodontics and for fabricating provisional 3D-printed restorations in clinics, various efforts have been made to reduce printing time; however, the impact on accuracy cannot be ignored. Recently, liquid crystal display (LCD) printers have become more cost-effective with increased resolution. In addition to the price advantage, LCD printers have the advantages of faster printing speed and less pixel distortion owing to the absence of light expansion by the projector lens [1–5].

Normal printing requires a resin with a viscosity of 1000 cPs or less. Moreover, the viscosity of the resin should be as low as possible to improve printing accuracy and reduce printing failure. Low-viscosity resins can improve the miscibility of raw materials, minimize the segregation and deposition of mixed materials, and improve mechanical properties while maintaining low viscosity by adding fillers. In addition, when the build platform moved during printing, fewer air bubbles formed in the bath, and the liquid resin quickly flowed into and filled the gaps between the layers, thereby increasing the printing speed. This allows for fine and accurate layer thickness control and provides a more dimensionally accurate output. Low-viscosity resins can also shorten the rinsing time after printing [6–9].

Previous studies have compared the accuracy of different types of 3D printers [10–27]. Kim et al. reported that the PolyJet technique was the most accurate [16], whereas Rebong et al. reported that fused deposition modeling (FDM) technology showed the least dimensional difference compared to the original model [10]. In addition, Park et al. compared printed models in the x, y, and z-axes and reported that FDM and DLP casts tended to shrink, whereas the Polyjet and SLA casts expanded buccolingually and anteroposteriorly [11]. Kim et al. reported that the post-polymerization shrinkage rate changed depending on the type of post-polymerization devices [28]. Joda et al. studied the change of accuracy according to the storage period after printing and found that 1 day of aging resulted in the highest accuracy [29]. As such, several studies evaluated the accuracy of different 3D printers by physically measuring or scanning and superimposing printed models [10–32]. However, few studies made quantitative comparisons with numerical reference data. Moon et al. and Tsolakis et al. reported that DLP 3D printers are more accurate than LCD 3D printers; however, a few research has been conducted on LCD printers [13,32,33].

Resolution describes the sharpness of a TV screen or computer display. The resolution in additive manufacturing, such as 3D printing, is expressed in the x-, y-, and z-axes and is primarily determined by the size of the laser spot, pixel size, and layer thickness. The XY resolutions of 2 K, 4 K, and 8 K 3D printers are approximately 53 μm, 35 μm, and 22 μm, respectively. Favero et al. studied the accuracy of SLA printers depending on the change in layer thickness, which represents the z-axis resolution, and reported that a smaller layer height, or shorter z-axis, did not always yield higher accuracy [7]. While some studies have compared accuracy based on layer height in SLA and DLP printers, few have compared accuracy according to the resolution in the x and y axes [34–39].

Although many studies have compared the accuracy of different 3D printers, they used different resins recommended by each 3D printer manufacturer, different conditions such as layer thickness, different post-polymerization times, and conditions by using different post-polymerization devices. Therefore, direct comparisons of the performances of 3D printers using one type of resin are required to control for independent variables.

This in vitro study aims to compare and evaluate the accuracy of full-arch models produced by 3D printers with various principles and resolutions using a low-viscosity resin. The dimensional accuracy and surface characteristics of both the entire arch and individual teeth were compared between the 3D printer groups. The null hypothesis was that there would be no significant differences in the

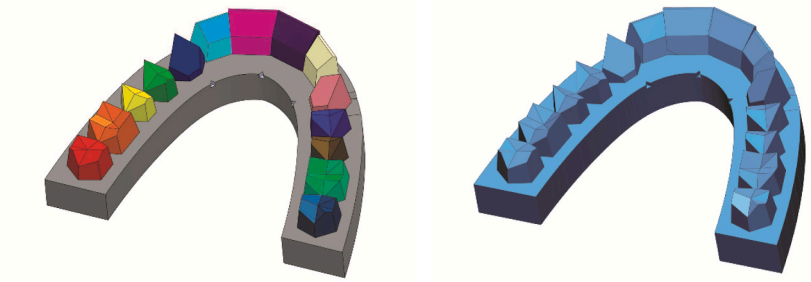

Fig. 1. Reference cast design. A. CAD design, and B. 3D printed cast.

accuracy among the different 3D printer groups.

2. Methods

A reference cast of the maxillary arch consisting of polygonal tooth shapes without curves was computer-aided design (CAD)-designed using Pro Engineer wildfire (ver. 5.0; PTC Inc) to enable measurements after 3D printing (Fig. 1(A) and B). The evaluated 3D printers were DLPa (Asiga MAX; Asiga), DLPk (Cara Print 4.0; KULZER), LCD2o (Ondemand 2 K Printer; Cybermed), LCD2p (Photon Mono X; Anycubic), LCD4s (SONIC 4 K; Phrozen), and SLA (ZENITH U; DENTIS). The characteristics of the 3D printer are listed in Table 1. Pre-processing, including support design and slicing, was performed according to the manufacturer's instructions. DLPa, DLPk, and SLA used the manufacturers' preprocessing software, whereas general-purpose software (CHITUBOX Basic; Chitubox) was used for LCD2o, LCD2p, and LCD4s. The cast was placed at the center of the build platform to print one cast per build platform, with the anterior part of the cast facing forward and the occlusal plane parallel to the build platform. While the shapes and densities of the supports, raft layers, and shapes were set according to the 3D printer manufacturers' instructions, efforts were made to match them as consistently as possible across 3D printers. Each layer was 100 μm thick. Before printing, all the 3D printers were calibrated by a single technician with more than five years of experience. Printing was performed 10 times using a light-curing resin for 3D printing (C&B Temporary; ODS Co., Ltd.) with a viscosity of approximately 500 cPs (Lot No. OCB01220218). The 3D printing parameters for this resin were determined by the information provided by the manufacturers [40]. The temperature and humidity in the 3D printer room were maintained at approximately 23 °C and 50 %, respectively. Each 3D printer was preheated for 30 min before printing, and the interval between the printing steps was set to 20 min to allow the 3D printer to cool fully. After printing, the cast was subjected to the following postprocessing procedures. Excess resin liquid was removed using a compressed air gun, followed by rinsing in an ultrasonic cleanser with 70 % isopropyl alcohol for 1 min and removing the alcohol with an air gun. Thereafter, the casts were placed in the open for 20 min to completely air dry excess alcohol and then post-polymerized for 7 min in a post-polymerization device (CURE BOX; ODS Co., Ltd.). To minimize dimensional changes, the printed casts were digitized using a desktop scanner (T710; Medit Co., Ltd.) within 24 h without powder application and saved as Stl files. To reduce interpersonal variation, all procedures were performed by a single researcher with more than one year of experience.

The accuracy of each 3D printer was evaluated by calculating the shell-to-shell deviation between the reference cast and 3D-printed casts using the root mean square (RMS) and qualitatively evaluating the color mapping. In addition, the deviation between the reference data and the measurements of the 3D-printed casts was evaluated for 12 linear, one angular, and five height items between the seven reference points from A to G (Figs. 2 and 3). The measurements were performed using 3D inspection software (Geomagic Control X; 3D Systems).

To evaluate the surface light reflection and external features of the 3D-printed casts, the labial side of the anterior part, the lingual side of the canine teeth, and the buccal and occlusal sides of the molars were photographed using a digital camera (D90; SONY). To evaluate the layering morphology and surface characteristics of the 3D-printed casts, three areas, including the lingual surface of the anterior part, the tip of the canine, and the central fossa of the molar, were photographed using FE-SEM (Apreo S; Thermo Fisher Scientific) at 250× magnification.

Statistical software was used for the analysis (IBM SPSS Statistics, v23.0; IBM Corp). The sample size was calculated using GPower (G*Power Ver 3.1.9.2.; Heinrich-Heine-Universität). For DLP, LCD, and SLA, approximate expected values for the median deviation of the measurements were assumed as 650 μm, 550 μm, and 500 μm, respectively, with a common standard deviation set at 90 μm [41]. The effect size was calculated to be 0.62. Utilizing this, with an alpha error set at 0.05 and power at 0.95, sample sizes were calculated for each group, with 10 samples per group and 60 samples across six groups [42]. Levene's test for variance equality and Shapiro–Wilk test for variable normality were performed for two main outcomes, RMS and median trueness value. While RMS satisfied the assumptions ($p > .05$), median trueness value did not ($p < .05$). The RMS values of shell-to-shell deviation between the reference cast and the 3D-printed casts were compared using one-way ANOVA and Tukey Honestly Significant Difference (HSD) tests. The median trueness values of the deviations between the reference data and the measurements of 3D printed casts were examined using Kruskal–Wallis tests, followed by Mann–Whitney U tests with Bonferroni adjustment for pairwise comparisons (Table 2). The statistical significance was set at $p < .05$.

Table 1
Specifications of 3D printers investigated.

System	Abbr.	Manufacturer	Technology	Build Volume(mm)	Light Source	XY resolution
Asiga MAX	DLPa	ASIGA	DLP	119x67x75	385 nm high-power UV LED	62 μm
cara Printer 4.0	DLPk	KULZER	DLP	103x58x130	9~9.9㎽/㎠, 405 nm UV light	53.6 μm
Ondemand 2K Printer	LCD2o	CYBERMED	LCD	82x130x150	405 nm arrayed LED/80W	51 μm
Photon Mono X	LCD2p	ANYCUBIC	LCD	192x120x245	3~3.24 ㎽/㎠, LED Panel	50 μm
SONIC 4K	LCD4s	PHROZEN	LCD	134.4x75.6x200	1.2–1.4 ㎽/㎠, LED Panel	35 μm
ZENITH U	SLA	DENTIS	SLA	110x110x150	Blue laser	90 μm

3D, 3-dimensional; DLP, digital light processing; LCD, liquid crystal display; SLA, stereolithography.

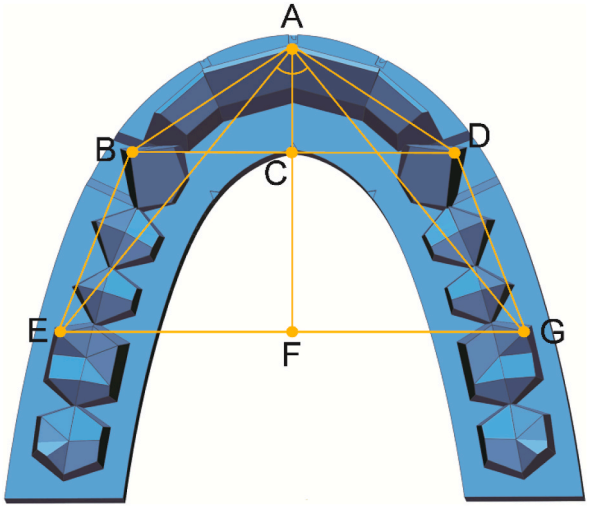

Fig. 2. Reference points, lines, and angulation on reference cast. $\overline{BD}$, intercanine width; $\overline{BC}$, right half of intercanine width; $\overline{CD}$, left half of the intercanine width; $\overline{EG}$, intermolar width; $\overline{EF}$, right half of the intermolar width; $\overline{FG}$, left half of the intermolar width; $\overline{AC}$, anterior arch length; $\overline{AF}$, total arch length; $\overline{AB}$, right anterior circumferential length; $\overline{AD}$, left anterior circumferential length; $\overline{BE}$, right posterior circumferential length; $\overline{DG}$, left posterior circumferential length; ∠EAG, arch convexity.

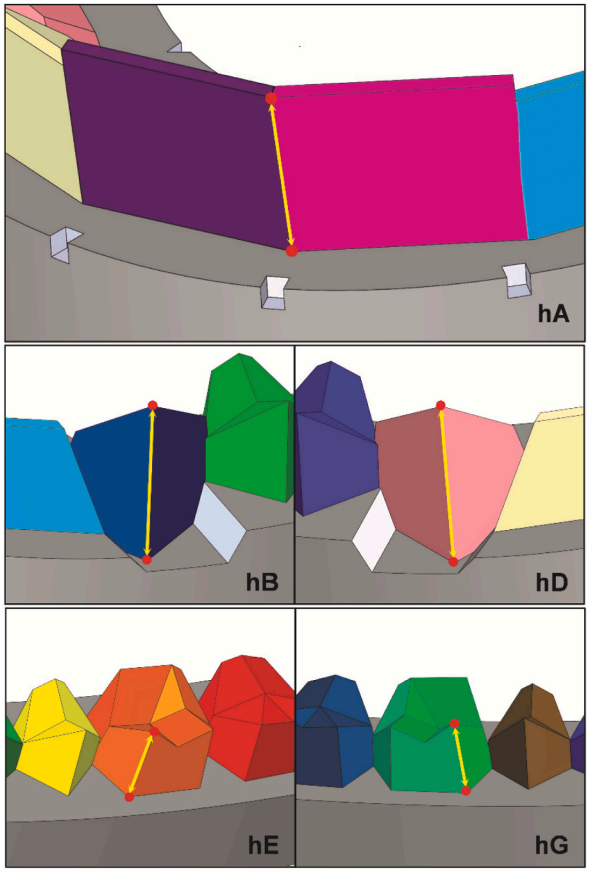

Fig. 3. Three-dimensional structure of individual tooth with measuring length. hA, height of the point between central incisors; hB, right canine height; hD, left canine height; hE, height of the mesiobuccal cusp of the right first molar; hG, height of the mesiobuccal cusp of the left first molar.

Table 2
Comparison of median deviations among 3D printed casts (unit: μm).

		DLPa	DLPk	LCD2o	LCD2p	LCD4s	SLA	*P*	df
Linear	$\overline{BD}$	375.10 [355.45,405.05]^{D}	469.40 [426.50,487.75]^{C}	823.90 [790.58,837.58]^{A}	619.15 [560.23,643.83]^{B}	455.85 [424.15,471.10]^{C}	530.90 [459.78,573.45]^{C}	<0.01	5
	$\overline{BC}$	63.45 [54.13,73.15]^{C}	106.30 [80.50,124.15]^{C}	350.75 [165.88,381.78]^{AB}	271.40 [252.45,289.68]^{A}	190.15 [157.95,258.93]^{B}	196.75 [141.48,225.00]^{B}	<0.01	5
	$\overline{CD}$	50.15 [41.78,63.38]^{D}	154.35 [93.40,165.70]^{CD}	356.90 [324.45,424.38]^{A}	244.10 [216.08,251.23]^{B}	101.65 [66.50,121.13]^{D}	159.45 [104.68,218.93]^{C}	<0.01	5
	$\overline{EG}$	471.00 [459.40,480.35]^{D}	575.45 [521.70,605.98]^{C}	1016.05 [937.80,1056.98]^{A}	768.45 [735.30,784.65]^{B}	557.65 [498.75,584.45]^{C}	525.30 [482.98,572.20]^{C}	<0.01	5
	$\overline{EF}$	144.65 [136.15,158.05]^{C}	218.55 [178.78,245.88]^{B}	532.55 [336.43,587.00]^{AB}	345.60 [331.55,402.30]^{A}	264.25 [217.15,305.58]^{B}	137.30 [104.05,180.48]^{C}	<0.01	5
	$\overline{FG}$	141.00 [130.30,163.25]^{D}	265.00 [191.53,288.73]^{C}	525.30 [488.18,574.48]^{A}	319.30 [290.68,338.48]^{B}	175.85 [122.38,210.15]^{CD}	161.60 [121.65,222.80]^{CD}	<0.01	5
	$\overline{AC}$	43.15 [37.83,46.65]^{C}	77.05 [71.63,83.13]^{B}	142.75 [118.00,158.08]^{A}	113.45 [100.08,133.75]^{A}	134.80 [123.95,154.13]^{A}	42.50 [24.58,54.38]^{C}	<0.01	5
	$\overline{AF}$	113.35 [108.68,118.78]^{D}	169.45 [140.85,177.20]^{C}	548.50 [474.98,577.00]^{A}	334.25 [324.23,345.88]^{B}	429.05 [421.40,451.05]^{A}	17.85 [10.83,68.55]^{E}	<0.01	5
	$\overline{AB}$	241.15 [188.83,261.58]^{D}	227.10 [207.93,242.40]^{D}	469.10 [439.40,515.55]^{A}	353.95 [335.73,428.93]^{B}	315.80 [282.00,339.45]^{C}	282.80 [266.65,317.05]^{C}	<0.01	5
	$\overline{AD}$	234.50 [195.70,258.98]^{C}	241.60 [221.65,258.80]^{D}	443.15 [417.83,468.70]^{A}	347.55 [307.45,361.60]^{B}	281.65 [238.53,330.03]^{BC}	271.85 [235.80,327.20]^{BCD}	<0.01	5
	$\overline{BE}$	110.00 [93.05,139.63]^{C}	106.70 [84.18,129.90]^{CD}	301.65 [254.70,327.53]^{A}	185.90 [182.20,206.85]^{B}	295.05 [255.88,318.35]^{A}	42.20 [14.78,97.85]^{D}	<0.01	5
	$\overline{DG}$	90.40 [71.60,115.55]^{C}	126.60 [81.98,157.40]^{C}	331.40 [289.45,354.03]^{A}	241.25 [201.58,250.75]^{B}	294.70 [255.18,306.60]^{A}	64.90 [28.95,91.55]^{C}	<0.01	5
Angular	∠EAG	0.15 [0.13,0.16]^{C}	0.29 [0.27,0.39]^{A}	0.24 [0.20,0.33]^{AB}	0.18 [0.15,0.23]^{BC}	0.22 [0.19,0.31]^{AB}	0.31 [0.26,0.35]^{A}	<0.01	5
Height	hA	33.50 [18.40,45.90]^{CD}	95.90 [78.20,103.30]^{B}	25.35 [6.65,45.15]^{D}	121.00 [105.05,134.10]^{A}	61.70 [45.13,103.70]^{B}	63.85 [30.85,83.58]^{BC}	<0.01	5
	hB	320.95 [311.10,334.98]^{C}	332.55 [306.98,343.18]^{C}	292.30 [281.85,345.23]^{C}	429.80 [413.15,450.48]^{B}	343.25 [311.38,372.45]^{C}	542.65 [489.03,595.25]^{A}	<0.01	5
	hD	319.95 [305.78,352.65]^{C}	308.05 [271.75,335.25]^{C}	270.75 [232.98,332.40]^{C}	381.50 [354.45,405.58]^{B}	323.85 [294.68,366.13]^{C}	478.85 [430.85,570.18]^{A}	<0.01	5
	hE	217.40 [209.98,230.73]^{C}	230.20 [204.38,246.25]^{C}	265.95 [243.08,318.80]^{AB}	317.35 [287.80,344.43]^{A}	232.85 [216.33,247.75]^{BC}	347.20 [311.70,369.30]^{A}	<0.01	5
	hG	226.40 [210.25,255.80]^{C}	232.55 [197.25,260.18]^{BC}	220.85 [187.50,234.30]^{C}	292.20 [255.58,314.45]^{B}	215.20 [191.68,242.05]^{C}	340.50 [307.30,368.80]^{A}	<0.01	5

df, degrees of freedom.
P, P-value from Kruskal-Wallis test.
Interquartile ranges [1st quartile, 3rd quartile] are in parentheses.
Different uppercase letters within the same row indicate statistical differences among 3D printers.
(multiple comparisons by Mann–Whitney *U* test with Bonferroni correction) ($P < .05$)Deviation denotes measurement minus the reference value of each evaluation item.
Statistical analysis was conducted using the absolute value of the deviation to prevent positive and negative measurements from canceling out, as the median values were calculated.

3. Results

The results of the evaluation of the shell-to-shell deviation are shown in Fig. 4. The DLPa and SLA printers had low trueness values, whereas the LCD printers had high trueness values. Among the LCD Printers, the LCD4s and LCD2o had the lowest and highest trueness values, respectively ($P < 0.01$). In the color-coded maps, the LCD2o group cast showed an increase in the height of the second molar area and a smaller buccal width, resulting in a narrow arch. (Fig. 5).

The measurement results for each cast are presented in Table 2 and Fig. 6(A-C). For the total linear deviation, DLPa exhibited the lowest trueness value, followed by SLA and DLPk. LCD printers showed high trueness values ($P < 0.01$). For intercanine and intermolar distances ($\overline{BD}$ and $\overline{EG}$), DLPa showed low trueness values, whereas LCD printers generally showed high trueness values, although LCD4s showed trueness values similar to those of SLA and DLPk ($P < 0.01$). Regarding the arch length ($\overline{AF}$), SLA had the lowest trueness value, followed by DLPa and DLPk ($P < 0.01$). The left-right difference ($\overline{BC}$, $\overline{CD}$ and $\overline{EF}$, $\overline{FG}$) of the 3D printed casts was large for the LCD4s ($P < 0.01$). Regarding angular deviation (∠EAG), DLPa had the lowest trueness value ($P < 0.01$). For the total height deviation, DLPa, DLPk, LCD2o, and LCD4s showed values in the 200 μm range, whereas LCD2p and SLA showed values in the 300 μm range ($P < 0.01$). The area with height deviation less than 100 μm was the anterior area (hA) ($P < 0.01$). The height deviations were largest in the canines (hB and hD), with LCD2o in the 200 μm range, DLPa, DLPk, and LCD4s in the 300 μm range, LCD2p in the 400 μm range, and SLA in the 500 μm range ($P < 0.01$). The deviations in the molars (hE and hG) were in the 200 μm range for DLPa, DLPk, LCD2o, and LCD4s, and in the 300 μm range for LCD2p and SLA ($P < 0.01$).

The surface characteristics of the 3D-printed casts photographed using a digital camera are shown in Fig. 7(A and B). Compared with other 3D printers, the casts from the SLA showed a greater degree of light reflection, and a small and sharp point, such as the tip of the canine, appeared blunt. In addition, the layered stepwise structure of the molar area is unclear.

The layer shapes of the 3D-printed casts observed using FE-SEM are shown in Fig. 8(A-C). The layers in the SLA appeared blurry and were connected smoothly. In the anterior lingual area, the borders of each layer were rough and uneven, except for those of DLPa and LCD4s. At the tip of the canine, LCD2o was printed to the last layer, whereas DLPa, DLPk, and LCD4s were printed to the second layer from the last layer. DLPa, DLPk, LCD2p, and LCD4s produced the deepest layer in the central fossa of the first molar, whereas the other two groups failed to print.

4. Discussion

The quantitative analysis in this study, including the shell-to-shell deviation and linear, angular, and height deviations, showed statistically significant differences between the 3D printer groups. Thus, the null hypothesis that there is no significant difference in accuracy between the different 3D printer groups was rejected.

In this study, SLA was the most accurate in terms of shell-to-shell deviation, which may be attributed to the high intensity of the laser spot, allowing sufficient polymerization between each layer. However, Im et al. found that DLP printers performed better than SLA printers, in contrast to our findings, likely owing to differences in the evaluated 3D printers between studies. We observed that the LCD printers printed less accurately, likely because the light intensity was not uniform, depending on the position of the LCD panel, and was not sufficiently strong. The SLA printer likely involves applying a sufficient output of UV light to the vat using a laser beam emitter, and the DLP printer projects a strong output of UV light through a DLP engine, whereas the LCD printer relies on the LED components of the panel, resulting in the observed differences. Morón-Conejo et al. compared the accuracy performance of industrial and dental desktop 3D printers and found comparable results for Form 2, a low-budget SLA device [43]. In a study evaluating the trueness and dimensional stability of abutment die models, the Shuffle, economic LCD 3D printer group showed the least trueness but was still comparable to the stone dies group [44].

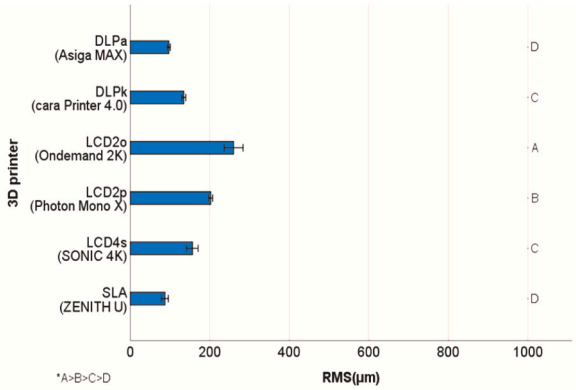

Fig. 4. Bar diagram showing the median values for trueness of shell-to-shell (reference versus printed casts) measured from scanned casts of each 3D printer group. Different uppercase letters on the right side indicate statistical differences among 3D printers ($P < 0.05$). RMS, root mean square; 3D, 3-dimensional; DLP, digital light processing; LCD, liquid crystal display; SLA, stereolithography.

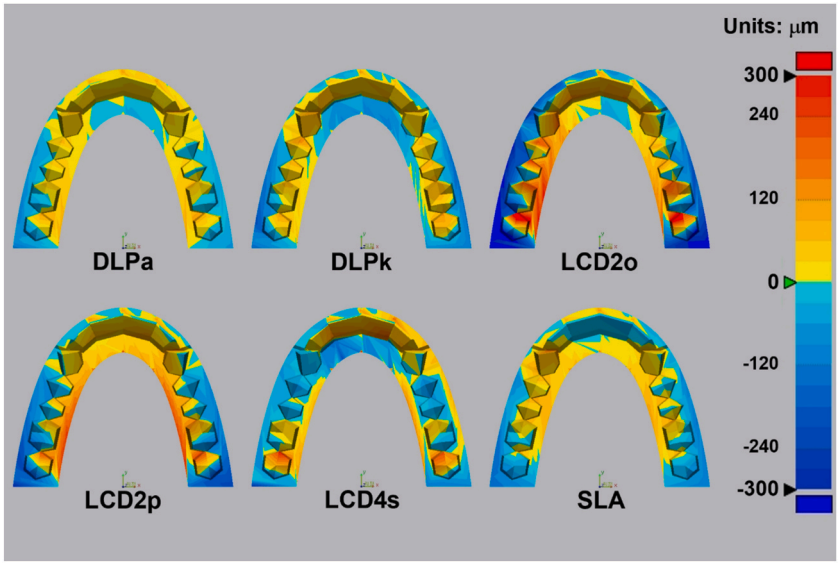

Fig. 5. Deviation of 3D printed casts relative to reference cast. The range of deviation was color-coded from −300 μm (blue) to 300 μm (red) and the allowable tolerance option was set to zero. DLP, digital light processing; LCD, liquid crystal display; SLA, stereolithography.

Regarding linear deviation, Nestler et al. found that DLP was more accurate than SLA, which is consistent with our findings [20]. This is likely because the raft of DLPa in this study touched the build platform up to the middle of the U-shape, resulting in less deformation during the post-polymerization process. The LCD printers were less accurate in all categories, which is consistent with the RMS results. DLPa was the most accurate for angular deviation, which was consistent with the findings of Camardella et al. who studied the accuracy of printed models based on the design of the model base [17]. Regarding height deviation, only the anterior part was less than 100 μm, possibly because the last layer of the anterior part was longer and wider than the other parts, resulting in stable printing up to the last layer. Small and pointed canine tips showed the largest deviation, with casts from the SLA being the least accurate. This is likely because the laser beam of the SLA printer evaluated in this study had a large size of 90 μm of the laser spot, which led to less polymerization of the small and sharp canine tip and a blurred border, resulting in less polymerization in the edge [3]. Eimir et al. reported excellent accuracy of SLA in the z-axis, in contrast to our study, possibly because the cylinders evaluated had flat and wide tips and the type and size of the laser spots differed [25]. Park et al. also reported a reduced z-axis in the SLA group, which was consistent with our study [11]. In contrast to the low trueness values in the RMS evaluation, SLA showed high trueness values in the z-axis evaluation items for accuracy in small and sharp areas, possibly due to the uniqueness of the shape of the reference cast used in this study.

The x–y resolution of each 3D printer represents the length of one side of a square pixel projected onto the build platform. The resolution varied even for the same 2 K 3D printers, depending on the number of pixels and the size of the build platform. The DLPa, which had the highest XY resolution of the 3D printers studied (62 μm), showed low trueness values for most items. The DLP groups were more accurate than the LCD groups in terms of RMS, likely because of the difference in photopolymerization type rather than resolution. This was consistent with the findings by Tsolakis et al. [32]. In shell-to-shell deviation, DLP printers were also more accurate, showing lower trueness values than LCD4s, suggesting that dimensional accuracy should be attributed more to the control of the photopolymerization by the printing principle rather than to the XY resolution of the 3D printers. However, among the LCD printers, the, 4 K 3D printer is more accurate than the 2 K 3D printer. This may be because a 4 K 3D printer has a higher resolution with more pixels, which allows for the concentration of light and better control over polymerization, resulting in a higher degree of polymerization. In addition, the hardware manufacturing technology affects the accuracy and quality of the outcome; thus, this aspect should be evaluated when choosing a low-cost 3D printer.

When the low-viscosity resin was used, no specimens failed to print, most of the residual monomers disappeared even after a 1-min rinsing, and no surface stickiness was observed on the printed cast. These advantages make low-viscosity resins an ideal reference material compatible with all evaluated 3D printers. Using this single-resin material, the independent variables were effectively minimized, focusing primarily on the 3D printing principles and resolution.

In the FE-SEM images, the casts from the SLAs showed smooth layer boundaries, which is a characteristic of the SLA, where the light intensity was weaker at the edges than at the center of the laser spot, and this was more pronounced when the laser beam was illuminated obliquely. In contrast, the casts from the DLPa and LCD4s showed clear differences between the layers, consistent with the findings of Park et al. [11]. On the lingual side of the anterior part, the casts from DLPk, LCD2o, and LCD2p had square borders for each layer, likely due to the appearance of corners of large pixels. At the tip of the small and pointed canine, DLPa, DLPk, and LCD4s produced smaller prints up to the last layer, likely due to full photopolymerization. The largest pixel size (62 μm) and less pronounced cascading of edge lines in the DLPa are likely due to antialiasing effects. The digital camera images were similar to those obtained using

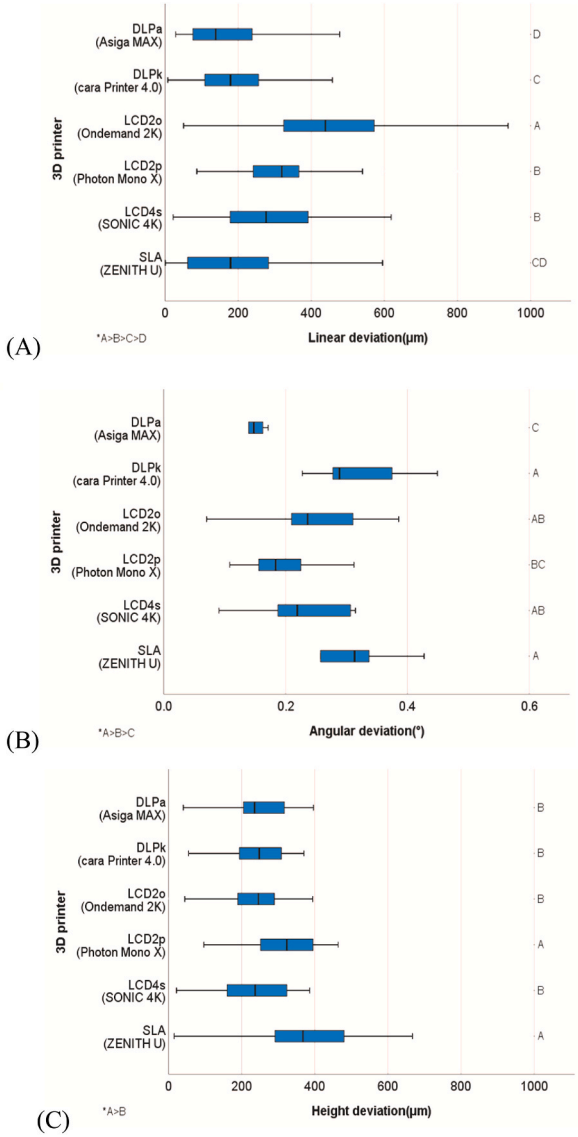

Fig. 6. Box plot diagram shows median values for trueness of distances and angulation measured from scanned casts of each 3D printer group. Different uppercase letters on the right side indicate statistical differences among 3D printers ($P < 0.01$). A. linear deviation, B. angular deviation, C. height deviation. 3D, 3-dimensional; DLP, digital light processing; LCD, liquid crystal display; SLA, stereolithography.

FE-SEM. Due to its smooth outer surface, we observed large light reflections at certain angles in the SLA, consistent with the findings of Park et al. [11]. In addition, the surface representation in the occlusal surfaces of molars and the slopes of the anterior teeth and molars appeared more detailed in LCD4s, likely due to the higher resolution.

It is important to produce a 3D printed model that is accurate to the appliance's fitting, such as occlusal bite, clear aligners, and wafers for orthognathic surgery [45]. Based on the results of this study, printers producing models with clear XY plane reproduction and less Z-direction distortion are recommended. The use of a high-resolution LCD panel is recommended when selecting a cost-effective LCD printer. A limitation of this study is that only the maxillary arch was represented in the test model. It would be beneficial to include models that address the different conditions encountered in clinical practice. Recently, DLP and LCD printers with enhanced resolutions of 4 K, 6 K, or 8 K have been introduced. Further research is required to evaluate the performance and accuracy of these 3D printers and compare the characteristics of low- and high-viscosity resins.

5. Conclusions

Based on the findings of this study, the following conclusions were drawn.

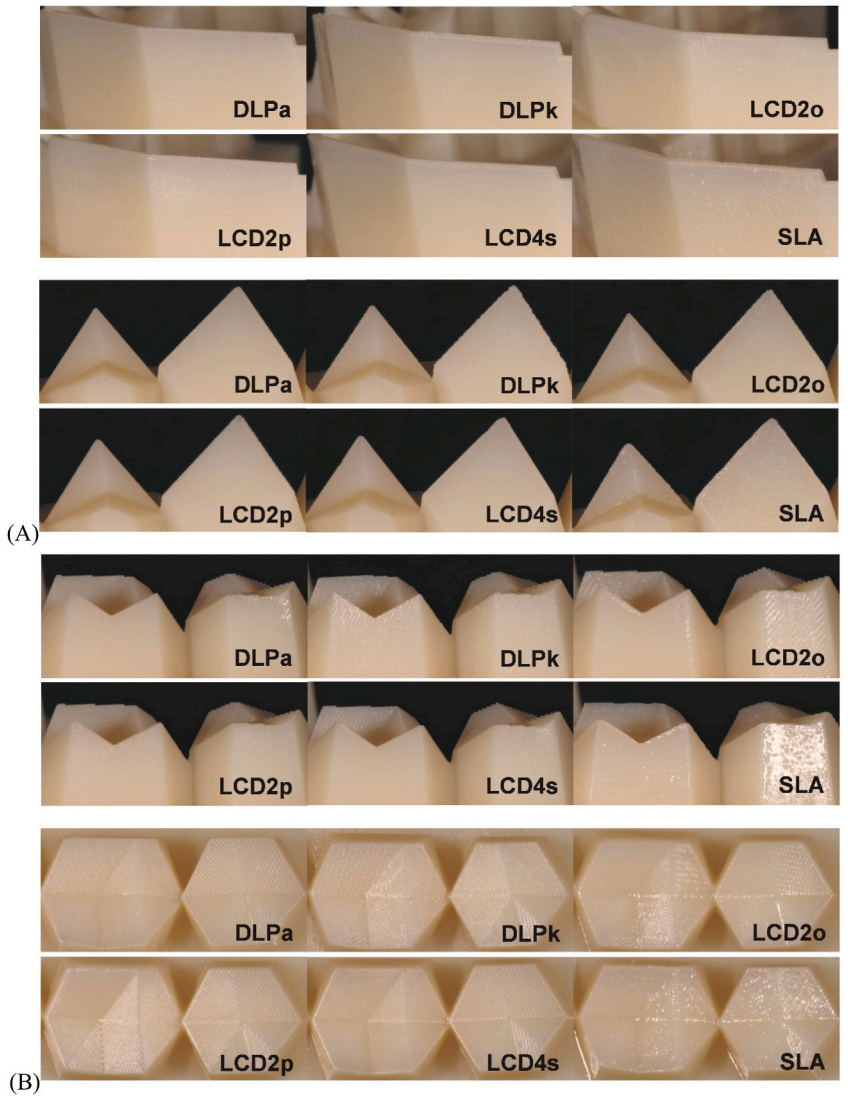

Fig. 7. Photographed casts at various angles. A. labial view of anterior teeth (upper) and lingual view of canine and premolar (lower), B. buccal view (upper) and occlusal view (lower) of molars. DLP, digital light processing; LCD, liquid crystal display; SLA, stereolithography.

1. The accuracy of 3D printed casts varied depending on the 3D printer group, in which DLPa and SLA were accurate in terms of shell-to-shell deviation, and DLPa was the most accurate in terms of linear and angular deviations.
2. Regardless of the XY resolution, DLP printers were more accurate than LCD printers. Among the LCD printers, LCD4s with higher XY resolution was more accurate.
3. The SLA showed smooth layer edges in FE-SEM owing to the characteristics of the laser spots and strong light reflection in the digital camera images. The high-resolution LCD4s showed more surface details in the digital camera images.

Data availability statement

The datasets used and/or analysed during the current study available from the corresponding author on reasonable request.

CRediT authorship contribution statement

Mi-Young Sim: Investigation, Writing – original draft. **June-Beom Park:** Writing – review & editing, Resources. **Deok-Yeoung Kim:** Resources, Writing – original draft. **Hae-Young Kim:** Formal analysis. **Ji-Man Park:** Writing – review & editing, Methodology, Conceptualization, Funding acquisition.

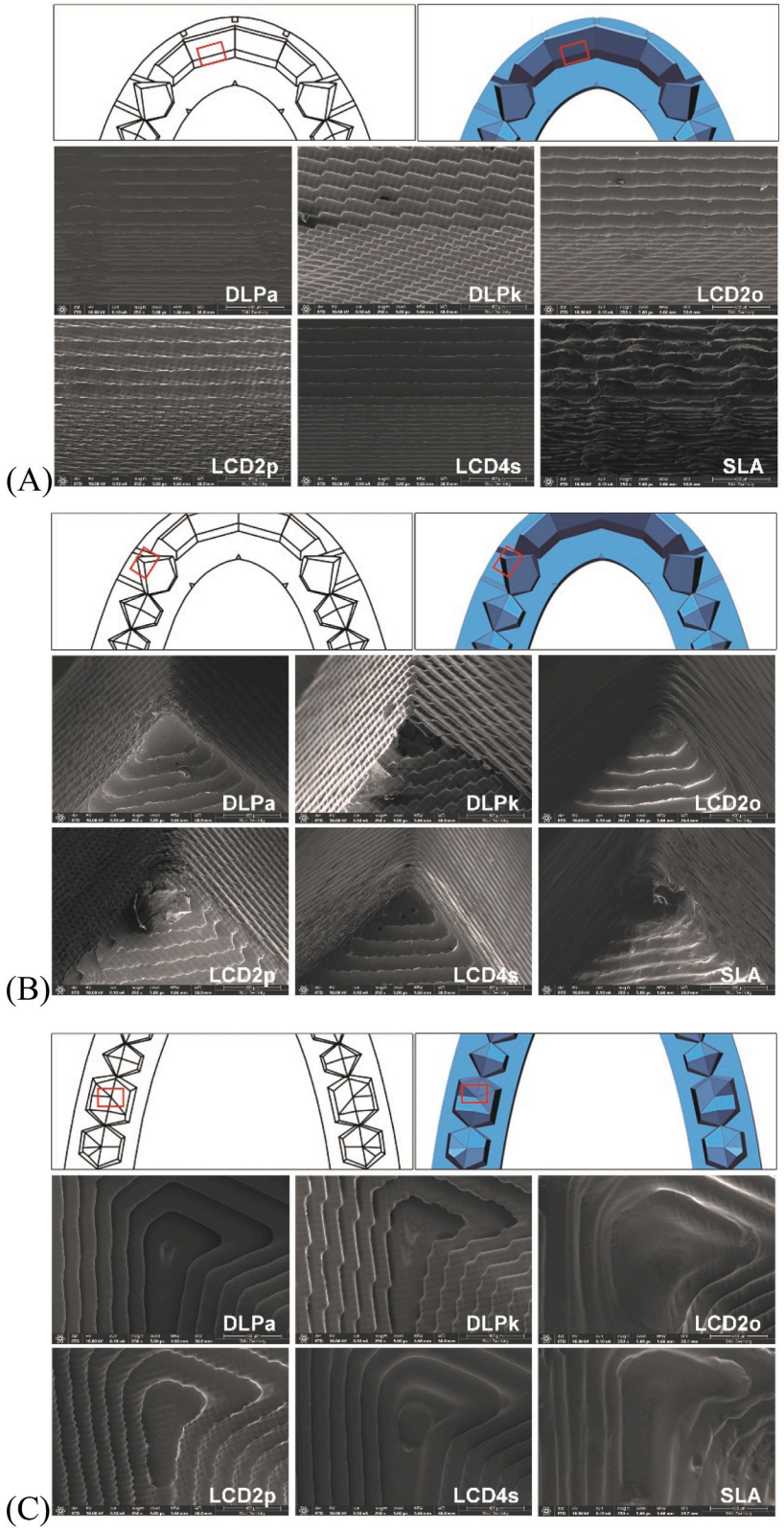

Fig. 8. FE-SEM(Field Emission Scanning Electron Microscope, Apreo S; Thermo Fisher Scientific) x250. A. lingual surface of the anterior part, B. tip of the canine, C. central fossa of the molar. DLP, digital light processing; LCD, liquid crystal display; SLA, stereolithography.

Declaration of competing interest

The authors declare the following financial interests/personal relationships which may be considered as potential competing interests: Ji-Man Park reports financial support was provided by Korea Medical Device Development Fund.

References

[1] H. Quan, T. Zhang, H. Xu, S. Luo, J. Nie, X. Zhu, Photo-curing 3D printing technique and its challenges, Bioact. Mater. 5 (2020) 110–115.
[2] I. Turkyilmaz, G.N. Wilkins, 3D printing in dentistry - exploring the new horizons, J. Dent. Sci. 16 (2021) 1037–1038.
[3] A. Reid, J. Windmill, Impact of beam shape on print accuracy in digital light processing additive manufacture, 3D Print. Addit. Manuf. (2023), 10:0.
[4] C.Y. Liaw, M. Guvendiren, Current and emerging applications of 3D printing in medicine, Biofabrication 9 (2017) 024102.
[5] A. Dawood, B. Marti Marti, V. Sauret-Jackson, A. Darwood, 3D printing in dentistry, Br. Dent. J. 219 (2015) 521–529.
[6] Z. Yang, S. Peng, Z. Wang, J.-T. Miao, L. Zheng, L. Wu, et al., UV-curable, low-viscosity resin with a high silica filler content for preparing ultrastiff, 3D-printed molds, ACS Appl. Polym. Mater. 4 (2022) 2636–2647.
[7] Y. Luo, G. Le Fer, D. Dean, M.L. Becker, 3D printing of poly(propylene fumarate) oligomers: evaluation of resin viscosity, printing characteristics and mechanical properties, Biomacromolecules 20 (2019) 1699–1708.
[8] F. Chen, R. Li, J. Sun, G. Lu, J. Wang, B. Wu, et al., Photo-curing 3D printing robust elastomers with ultralow viscosity resin, J. Appl. Polym. Sci. 138 (2021) 49965.
[9] D. Mostafavi, M.M. Methani, W. Piedra-Cascon, A. Zandinejad, M. Revilla-Leon, Influence of the rinsing postprocessing procedures on the manufacturing accuracy of vat-polymerized dental model material, J. Prosthodont. 30 (2021) 610–616.
[10] R.E. Rebong, K.T. Stewart, A. Utreja, A.A. Ghoneima, Accuracy of three-dimensional dental resin models created by fused deposition modeling, stereolithography, and Polyjet prototype technologies: a comparative study, Angle Orthod. 88 (2018) 363–369.
[11] J.M. Park, J. Jeon, J.Y. Koak, S.K. Kim, S.J. Heo, Dimensional accuracy and surface characteristics of 3D-printed dental casts, J. Prosthet. Dent 126 (2021) 427–437.
[12] C.H. Im, J.M. Park, J.H. Kim, Y.J. Kang, J.H. Kim, Assessment of compatibility between various intraoral scanners and 3D printers through an accuracy analysis of 3D printed models, Materials 13 (2020) 4419.
[13] W. Moon, S. Kim, B.S. Lim, Y.S. Park, R.J. Kim, S.H. Chung, Dimensional accuracy evaluation of temporary dental restorations with different 3D printing systems, Materials 14 (2021) 1487.
[14] K.C. Oh, J.M. Park, J.S. Shim, J.H. Kim, J.E. Kim, J.H. Kim, Assessment of metal sleeve-free 3D-printed implant surgical guides, Dent. Mater. 35 (2019) 468–476.
[15] M.E. Park, S.Y. Shin, Three-dimensional comparative study on the accuracy and reproducibility of dental casts fabricated by 3D printers, J. Prosthet. Dent 119 (2018) 861 e1–e7.
[16] S.Y. Kim, Y.S. Shin, H.D. Jung, C.J. Hwang, H.S. Baik, J.Y. Cha, Precision and trueness of dental models manufactured with different 3-dimensional printing techniques, Am. J. Orthod. Dentofacial Orthop. 153 (2018) 144–153.
[17] L.T. Camardella, O. de Vasconcellos Vilella, H. Breuning, Accuracy of printed dental models made with 2 prototype technologies and different designs of model bases, Am. J. Orthod. Dentofacial Orthop. 151 (2017) 1178–1187.
[18] S. Akyalcin, P. Rutkowski, M. Arrigo, C.A. Trotman, F.K. Kasper, Evaluation of current additive manufacturing systems for orthodontic 3-dimensional printing, Am. J. Orthod. Dentofacial Orthop. 160 (2021) 594–602.
[19] A. Hazeveld, J.J. Huddleston Slater, Y. Ren, Accuracy and reproducibility of dental replica models reconstructed by different rapid prototyping techniques, Am. J. Orthod. Dentofacial Orthop. 145 (2014) 108–115.
[20] N. Nestler, C. Wesemann, B.C. Spies, F. Beuer, A. Bumann, Dimensional accuracy of extrusion- and photopolymerization-based 3D printers: in vitro study comparing printed casts, J. Prosthet. Dent 125 (2021) 103–110.
[21] G.B. Brown, G.F. Currier, O. Kadioglu, J.P. Kierl, Accuracy of 3-dimensional printed dental models reconstructed from digital intraoral impressions, Am. J. Orthod. Dentofacial Orthop. 154 (2018) 733–739.
[22] W.N. Wan Hassan, Y. Yusoff, N.A. Mardi, Comparison of reconstructed rapid prototyping models produced by 3-dimensional printing and conventional stone models with different degrees of crowding, Am. J. Orthod. Dentofacial Orthop. 151 (2017) 209–218.
[23] O. Rungrojwittayakul, J.Y. Kan, K. Shiozaki, R.S. Swamidass, B.J. Goodacre, C.J. Goodacre, et al., Accuracy of 3D printed models created by two technologies of printers with different designs of model base, J. Prosthodont. 29 (2020) 124–128.
[24] K. Murugesan, P.A. Anandapandian, S.K. Sharma, M. Vasantha Kumar, Comparative evaluation of dimension and surface detail accuracy of models produced by three different rapid prototype techniques, J. Indian Prosthodont. Soc. 12 (2012) 16–20.
[25] F. Emir, S. Ayyildiz, Accuracy evaluation of complete-arch models manufactured by three different 3D printing technologies: a three-dimensional analysis, J Prosthodont Res 65 (2021) 365–370.
[26] S.J. Jin, I.D. Jeong, J.H. Kim, W.C. Kim, Accuracy (trueness and precision) of dental models fabricated using additive manufacturing methods, Int. J. Comput. Dent. 21 (2018) 107–113.
[27] K.Y. Lee, J.W. Cho, N.Y. Chang, J.M. Chae, K.H. Kang, S.C. Kim, et al., Accuracy of three-dimensional printing for manufacturing replica teeth, Korean J Orthod 45 (2015) 217–225.
[28] J.H. Kim, J.S. Kwon, J.M. Park, L. Lo Russo, J.S. Shim, Effects of postpolymerization conditions on the physical properties, cytotoxicity, and dimensional accuracy of a 3D-printed dental restorative material, J. Prosthet. Dent 3913 (2022) 281–285.
[29] T. Joda, L. Matthisson, N.U. Zitzmann, Impact of aging on the accuracy of 3D-printed dental models: an in vitro investigation, J. Clin. Med. 9 (2020) 1436.
[30] H. Chen, D.H. Cheng, S.C. Huang, Y.M. Lin, Comparison of flexural properties and cytotoxicity of interim materials printed from mono-LCD and DLP 3D printers, J. Prosthet. Dent 126 (2021) 703–708.
[31] M. Reymus, B. Stawarczyk, In vitro study on the influence of postpolymerization and aging on the Martens parameters of 3D-printed occlusal devices, J. Prosthet. Dent 125 (2021) 817–823.
[32] I.A. Tsolakis, W. Papaioannou, E. Papadopoulou, M. Dalampira, A.I. Tsolakis, Comparison in terms of accuracy between DLP and LCD printing technology for dental model printing, Dent. J. 10 (2022) 181.
[33] I.A. Tsolakis, S. Gizani, N. Panayi, G. Antonopoulos, A.I. Tsolakis, Three-dimensional printing technology in orthodontics for dental models: a systematic review, Children 9 (2022) 1106.
[34] Z.C. Zhang, P.L. Li, F.T. Chu, G. Shen, Influence of the three-dimensional printing technique and printing layer thickness on model accuracy, J. Orofac. Orthop. 80 (2019) 194–204.
[35] Y. Etemad-Shahidi, O.B. Qallandar, J. Evenden, F. Alifui-Segbaya, K.E. Ahmed, Accuracy of 3-dimensionally printed full-arch dental models: a systematic review, J. Clin. Med. 9 (2020) 3357.
[36] S.L. Sherman, O. Kadioglu, G.F. Currier, J.P. Kierl, J. Li, Accuracy of digital light processing printing of 3-dimensional dental models, Am. J. Orthod. Dentofacial Orthop. 157 (2020) 422–428.
[37] W.A. Loflin, J.D. English, C. Borders, L.M. Harris, A. Moon, J.N. Holland, et al., Effect of print layer height on the assessment of 3D-printed models, Am. J. Orthod. Dentofacial Orthop. 156 (2019) 283–289.
[38] J. Ko, R.D. Bloomstein, D. Briss, J.N. Holland, H.M. Morsy, F.K. Kasper, et al., Effect of build angle and layer height on the accuracy of 3-dimensional printed dental models, Am. J. Orthod. Dentofacial Orthop. 160 (2021) 451–458 e2.

[39] C.S. Favero, J.D. English, B.E. Cozad, J.O. Wirthlin, M.M. Short, F.K. Kasper, Effect of print layer height and printer type on the accuracy of 3-dimensional printed orthodontic models, Am. J. Orthod. Dentofacial Orthop. 152 (2017) 557–565.
[40] S. Zinelis, N. Panayi, G. Polychronis, S.N. Papageorgiou, T. Eliades, Comparative analysis of mechanical properties of orthodontic aligners produced by different contemporary 3D printers, Orthod. Craniofac. Res. 25 (2022) 336–341.
[41] J.H. Kim, K.B. Kim, W.C. Kim, J.H. Kim, H.Y. Kim, Accuracy and precision of polyurethane dental arch models fabricated using a three-dimensional subtractive rapid prototyping method with an intraoral scanning technique, Korean J Orthod 44 (2014) 69–76.
[42] H.Y. Kim, Statistical notes for clinical researchers: sample size calculation 3: Comparison of several means using one-way ANOVA, Restor Dent Endod 41 (2016) 231–234.
[43] Conejo B. Moron, J. Lopez Vilagran, D. Caceres, S. Berrendero, G. Pradies, Accuracy of five different 3D printing workflows for dental models comparing industrial and dental desktop printers, Clin. Oral Invest. 27 (2023) 2521–2532.
[44] Y.C. Lai, C.C. Yang, J.A. Levon, T.G. Chu, D. Morton, W.S. Lin, The effects of additive manufacturing technologies and finish line designs on the trueness and dimensional stability of 3D-printed dies, J. Prosthodont. 32 (2023) 519–526.
[45] Y. Wang, P. Wang, X. Xiang, H. Xu, Y. Tang, Y. Zhou, et al., Effect of occlusal coverage depths on the precision of 3D-printed orthognathic surgical splints, BMC Oral Health 22 (2022) 218.